# Mechano-chemical feedback leads to cell competition for cell fate specification

Daniel, J. Toddie-Moore[1¶*], Martin, P. Montanari[1], Isaac Salazar-Ciudad[1,2,3] and Osamu Shimmi[1,4*]

[1]Institute of Biotechnology, University of Helsinki, 00014 Helsinki, Finland

[2]Genomics, Bioinformatics and Evolution. Departament de Genètica i Microbiologia, Universitat Autònoma de Barcelona, 08193, Cerdanyola del Vallès, Spain

[3]Centre de Rercerca Matemàtica, 08193, Cerdanyola del Vallès, Spain

[4]Institute of Molecular and Cell Biology, University of Tartu, 51010 Tartu, Estonia

[*]Corresponding authors:

d.toddie-moore@ed.ac.uk and osamu.shimmi@helsinki.fi

[¶]Present address: University of Edinburg, United Kingdom

## Abstract

Developmental patterning is thought to be regulated by conserved signalling pathways. Initial patterns are often broad before refining to only those cells that commit to a particular fate[1,2]. However, the mechanisms by which pattern refinement takes place remain to be addressed. Using the posterior crossvein (PCV) of the *Drosophila* pupal wing as a model, into which bone morphogenetic protein (BMP) ligand is extracellularly transported to instruct vein patterning[3,4], we investigate how pattern refinement is regulated. We found that BMP signalling induces apical enrichment of Myosin II in developing crossvein cells to regulate apical constriction. Live imaging of cellular behaviour indicates that changes in cell shape are dynamic and transient, only being maintained in those cells that retain vein fate after refinement. Disrupting cell shape changes throughout the PCV inhibits pattern refinement. In contrast, disrupting cell shape in only a subset of vein cells can result in a loss of BMP signalling. We propose that cell shape changes of future PCV cells allow them to compete more efficiently for basally localised BMP signal by forming a mechano-chemical feedback loop. This study highlights a new form of cell competition: competing for a signal that induces cell fate rather than promotes cell survival.

## Main

Pattern formation is a fundamental process in animal development, for which various molecular mechanisms have been proposed, including gene regulatory networks and growth factor signalling[1,2]. Developmental patterning often involves refinement from a broad initial area of competency for a fate to only those cells that commit to it, with neighbours losing competence and following an alternate fate path (Fig. 1a)[1,2]. Whilst some mechanisms of pattern refinement, such as transcriptional networks and lateral inhibition, have previously been investigated, the role played by

39 diffusible growth factor signalling, in particular the interactions between signalling and
40 morphogenesis, has been less explored[5,6].

41 The PCV of the *Drosophila* pupal wing serves as an excellent model to address the dynamics of
42 signalling and morphogenesis, as its formation is initially directed by a single signalling pathway:
43 BMP signalling[4,7]. The *Drosophila* BMP ligand Decapentaplegic (Dpp) is initially expressed in the
44 adjacent longitudinal veins (LVs) and is extracellularly transported into the prospective PCV region
45 along the basal surfaces of the two cell layers that comprise the wing epithelia (Fig. 1b)[3]. BMP
46 signalling induced by the Dpp ligand forms the PCV field by becoming competent for vein, rather
47 than intervein fate (Fig. 1c). Continuous extracellular Dpp transport seems to be crucial for a period
48 of around 10 hours (18 – 28 h after pupariation (AP)) to maintain the PCV field and vein fate
49 competence, before PCV cells begin to express the ligand themselves[7]. Continued extracellular
50 signalling and vein morphogenesis occur concurrently, as morphogenesis begins shortly after BMP
51 signalling is activated[4]. Refinement of the BMP signalling pattern during this time window has
52 previously been observed; however how pattern refinement takes place has not been addressed[8].

53 **BMP signal induces cell shape changes**

54 First, we confirmed that refinement of the PCV field takes place during morphogenesis. The PCV
55 field is defined as the cells in which BMP signalling occurs, as indicated by staining with anti-
56 phosphorylated Mad antibody (pMad)[9], and which are therefore competent to assume a vein fate.
57 Our data reveal that the number of cells within the PCV field reduces between 20h AP, shortly after
58 the initiation of PCV patterning, and 28h AP, when PCV cells express *dpp* themselves (Fig. 1d, e).
59 Thus we term the period from 20 to 28 hours AP the 'refinement period'.

60 During this period, apical constriction of vein cells appears to be the hallmark of vein
61 morphogenesis[8,10]. Since BMP signalling is thought to initiate PCV development[3], we next asked
62 whether BMP signalling directs the wing vein-like cell shape changes (thereafter referring as "cell

63 shape changes") that occur during PCV morphogenesis. To answer this question, we captured
64 images of apical cell shapes in *crossveinless* mutant wings, where BMP signalling is inactive in the
65 PCV region, and observed that apical constriction does not occur (Fig. 1f)[11]. These results indicate
66 that BMP signalling is required for the cell shape changes that occur during PCV morphogenesis.

67 The activity of Myosin II (MyoII) has been proposed to be the driving force behind cell shape
68 dynamics such as apical constriction[12]. To investigate whether BMP signalling directs cell shape
69 change through MyoII activity, we analysed the spatial localisation of MyoII using MyoII
70 regulatory light chain (MRLC) tagged with RFP in wild type and *crossveinless* pupal wings[13]. In
71 wildtype wings, MyoII is enriched in the apical compartment of PCV cells, with lower basal levels,
72 but in contrast, neighbouring intervein cells have lower apical levels of MyoII than the PCV (Fig.
73 1g, Extended Data Fig. 1a). Conversely, in *crossveinless* pupal wings, apical MyoII enrichment is
74 not observed in the PCV region, although apical enrichment of MyoII is still detected in LVs (Fig.
75 1g, Extended Data Fig. 1a). These findings suggest that BMP signalling facilitates the apical
76 localisation of MyoII to promote apical constriction of PCV cells. This was further confirmed by
77 the observation that ectopic expression of the constitutively active form of BMP type I receptor in
78 mosaic analysis with a repressible cell marker (MARCM) clones within the pupal wing induces
79 apical enrichment of MyoII, as well as strong apical constriction (Extended Data Fig. 1b)[8,14].

80 **Time lapse imaging during vein morphogenesis**

81 As wing vein morphogenesis directed by BMP signalling and refinement of the BMP signalling
82 pattern occur concurrently, we hypothesised that these events could be mutually coordinated. To
83 address this, we employed *in vivo* live imaging of pupal wings expressing GFP tagged E-cadherin to
84 observe cell shape changes during the refinement period[15]. We tracked the apical shapes of cells
85 that are part of the PCV at the end of the refinement period, and thus retained vein fate, and
86 compared it to the cells flanking this region (Fig. 2a-c, Supplementary Videos 1-3). Intriguingly,

87 whilst the cells which will form the PCV apically constrict throughout the refinement period,
88 several of the cells immediately flanking these constrict apically at early time points but fail to
89 maintain their vein-like morphology at later time points, eventually reverting to an intervein fate
90 (Fig. 2a-c, Supplementary Videos 1, 2).

91 **Cell shape change and pattern refinement**

92 We hypothesised that cell shape changes themselves may affect signalling pattern refinement and
93 thus cell fate choice in the PCV region (Fig. 2d). To test this idea, we modulated cell shape changes
94 in the developing wing by attenuating MyoII activity using a dominant negative form of the Myosin
95 Heavy Chain (MyoII-DN)[16]. Inhibiting MyoII activity across the posterior wing blade for 10 hours
96 during PCV morphogenesis is sufficient to disrupt apical constriction in the PCV region and LV
97 cells of 25h AP pupal wings (Extended Data Fig. 2a). Intriguingly, loss of MyoII activity
98 throughout posterior wing results in a broader range of BMP signalling in the PCV region than in
99 control wings, suggesting that cell shape changes are necessary for the refinement of the BMP
100 signalling but not for BMP signalling itself (Fig. 3a, b). Additionally BMP signalling is missing in
101 the PCV region when MyoII activity was disrupted in the posterior half of wings of *crossveinless*
102 background, indicating that the unrefined BMP signalling pattern is still being directed by
103 extracellular BMP signalling (Extended Data Fig 2b).

104 What then is the role of cell shape changes in signalling pattern refinement? Despite reversal of
105 BMP-induced cell shape changes being associated with reduced competence for vein fate, blocking
106 cell shape changes did not affect BMP signalling. We hypothesised that what might be important is
107 not cell shape change itself, but how cell morphology compares to that of other cells within the
108 field. The impact of cell shape change loss may then be context specific, facilitating refinement by
109 causing less signalling and fate loss in cells surrounded by those with greater changes in shape. If
110 this the case, inhibition of cell shape changes in a small group of cells within the PCV field may

111 decrease their ability to retain BMP signalling and vein fate. We tested this hypothesis by
112 generating clones that attenuate cell shape changes amongst neighbours that are wild type.
113 Strikingly, when MyoII attenuated clones are produced within the PCV field, loss of BMP
114 signalling can often be observed in context dependent manner (Fig. 3c, Extended Data Fig. 2c).
115 This suggests that MyoII-based cell shape changes play a crucial role in whether a cell retains vein
116 fate during refinement, despite not being required for competency for BMP signalling. When all
117 PCV field cells cannot form vein-like shapes, signalling still occurs throughout and refinement does
118 not take place (Fig. 3a, b, d, Extended Data Fig. 4b). However, when cells are present in a
119 heterogeneous population with or without cell shape changes, cells that can change shape both
120 retain the signal and acquire vein fate (Fig. 3c, d, Extended Data Fig. 4b). We propose that this
121 represents a novel type of cell competition; where the outcome instructs cell fate determination
122 rather than survival or elimination (Fig. 2d, Extended Data Fig. 4a, b). Winner cells are those within
123 the field that retain cell shape changes and acquire vein fate by maintaining BMP signalling,
124 whereas loser cells are less competitive for the BMP signal, resulting in the inability to retain shape,
125 and revert to intervein fate (Extended Data Fig. 4). Furthermore, our data indicate that the
126 mechanism of pattern refinement is a mechano-chemical feedback loop as BMP signalling induces
127 the cell shape changes, which in turn influence the ability of cells to retain that signal.

128 **Basal cell shape and cell competition**

129 We next considered what the mechanism of cell shape change-mediated cell competition could be.
130 Previous studies indicate that extracellularly trafficked Dpp ligands are predominantly localised on
131 the basal side of the wing epithelia[3]. Since BMP receptor appears to be down-regulated by BMP
132 signalling throughout wing development, expression of receptors may not explain the
133 mechanism[3,17]. Thus, we hypothesized that expansion in basal cell size may increase
134 competitiveness for capturing basal ligand within the signalling microenvironment, resulting in
135 producing winner cells. We therefore investigated the basal size dynamics of PCV field cells[3]. We

136 observed that cells at the periphery of the PCV field (that lose their fate during refinement) are
137 consistently smaller than those at the centre of the field during the refinement period (Fig. 4a, b).

138 To examine whether differential basal cell size is a mechanism by which cell competition for cell
139 fate could occur, we observed whether differences in basal cell size within the PCV field are still
140 observed when refinement does not take place due to attenuated MyoII activity. We observed that
141 unlike wild type wings differences in basal cell surface between central and peripheral cells are not
142 observed when MyoII activity is disrupted in the posterior half of pupal wing (Extended Data Fig
143 3a). These data are consistent with basal cell size dynamics playing a role in the mechanism of cell
144 competition-mediated refinement.

145 Furthermore, we found that the basal surfaces of *crossveinless* cells do not expand in the region
146 between L4 and L5 where the PCV field should form, suggesting that BMP signalling plays a
147 positive role in the basal expansion of these cells (Extended Data Fig. 3b). Considering that BMP
148 signalling induces apical but not basal enrichment of MyoII in the PCV region (Fig. 1g, Extended
149 Data Fig. 1a), it is likely that BMP induced apical constriction is important for changes in basal
150 shape and forms a mechano-chemical feedback loop facilitating cell competition for cell fate, which
151 lead to pattern refinement.

152 **Discussion**

153 Here we found that cell shape changes are coupled to the refinement of BMP signalling during PCV
154 morphogenesis. Our findings reveal that cell shape changes drive refinement by directing
155 competition for the vein fate-determining BMP ligand, with loser cells acquiring intervein cell fate.
156 Previous studies have proposed that competition between cells for BMP signalling instructs the
157 pattern of survival and elimination in the *Drosophila* wing imaginal disc[18-20]. Since BMP signalling
158 is one of the key players regulating cell proliferation in the larval wing imaginal disc[21,22], cells
159 lacking BMP signalling are less proliferative than neighbouring cells and are eliminated as loser

160 cells (Extended Data Fig. 4)[23]. Although BMP still serves as a proliferative signal in the *Drosophila*
161 wing during the early pupal stage[24,25], BMP turns into a cell differentiation factor at the beginning
162 of the refinement period and thus competition has a different outcome. Therefore, competition for
163 the BMP signal leads to winner and loser cells acquiring different cell fates (vein or intervein) in
164 later pupal development (Extended Data Fig. 4).

165 Our data suggest that dynamic basal cell shape changes are important for the determination of
166 winner and loser cells and may allow PCV field cells to better compete for extracellular ligand or
167 space within the signalling micro-environment. Although BMP signalling is needed for cell shape
168 changes to occur, the differences in basal cell dynamics within the PCV field may not be directly
169 regulated by BMP signalling. Although previous studies have shown that BMP signalling induces
170 the expression of several molecules in the PCV region to optimize the BMP signalling by forming a
171 feedback loop[4,8,26], the expression of these factors begins from the early refinement stage and thus
172 initial differential transcription is unlikely to instruct differences in basal shape dynamics. They
173 may instead play a role in amplifying differences in the levels of BMP signalling between winner
174 cells and loser cells during refinement.

175 Changes in the 3D architecture of the pupal wing epithelia, such as apposition of the two wing
176 layers, are also unlikely to be responsible for differences in basal cell size. Unlike our recent
177 observations that the 3D architecture of pupal wing epithelia and BMP signalling in the LVs are
178 coupled[24], PCV refinement appears to be a 2D phenomenon as large single layer clones expressing
179 MyoII-DN that disrupt 3D architecture have been observed which do not affect refinement in the
180 other layer (Extended Data Fig. 2d). We rather consider that a cellular mechanical network within
181 the PCV field may trigger the differences in basal dynamics[5,6,27,28], therefore we propose that the
182 formation of differential basal dynamics during refinement is a self-organising process[2]. Further
183 study is needed to fully understand how basal cell shape dynamics are regulated during cell
184 competition.

185 We suspect that cell competition for cell fate is likely to be a general mechanism for self-
186 organisation of pattern refinement during development. Cell shape changes are a common part of
187 the morphogenesis programme and could feed back into developmental patterning in a variety of
188 contexts[5,6]. Apical constriction and basal expansion are an important aspect of epithelial folding, a
189 process which has broadly been linked to cell fate decisions and developmental patterning[5,6,29,30].
190 Our finding that cell shape changes within the 2D epithelial layer, irrespective of epithelial folding,
191 can instruct pattern refinement provides a novel insight into epithelial morphogenesis.

192 In summary, our data reveal that cell shape changes influence refinement of the signalling pattern
193 by facilitating cell competition for signalling pathway activation. We have uncovered that cell
194 competition occurs via a mechano-chemical feedback loop between cell shape changes and BMP
195 signalling, leading to self-organising refinement of the developmental field during pattern
196 formation.

197

198 **Acknowledgements**

199 We are grateful to Jukka Jernvall and Yukitaka Ishimoto for thoughtful comments on the
200 manuscript. We thank Light microscopy Unit, University of Helsinki for their support. We thank H.
201 Ohkura, R. Le Borgne, D. Kiehart and A. Martin for fly stocks. This work was supported by grant
202 308045 from the Academy of Finland, the Sigrid Juselius Foundation to O.S., grant 295013 from
203 the Academy of Finland to D.T-M., and the Center of Excellence in Experimental and
204 Computational Developmental Biology from the Academy of Finland to O.S. and I.S-C.

205

206 **Author contributions**

D.T-M. and O.S. conceived the project and planned experiments. D.T-M. and M.M. performed all experiments. D.T-M. analysed the results and discussed them with O.S. I.S-C. provided inputs. D.T-M. and O.S. wrote the manuscript and all authors made comments. O.S. supervised the project.

## Declaration of interests

The authors declare no competing interest.

## Data availability

Source Data for Figs. 1e, 2b, 3b, 4b are provided with the paper.

## References


1 Morelli, L. G., Uriu, K., Ares, S. & Oates, A. C. Computational approaches to developmental patterning. *Science* **336**, 187-191, doi:10.1126/science.1215478 (2012).

2 Schweisguth, F. & Corson, F. Self-Organization in Pattern Formation. *Dev Cell* **49**, 659-677, doi:10.1016/j.devcel.2019.05.019 (2019).

3 Matsuda, S. & Shimmi, O. Directional transport and active retention of Dpp/BMP create wing vein patterns in Drosophila. *Dev Biol* **366**, 153-162, doi:10.1016/j.ydbio.2012.04.009 (2012).

4 Matsuda, S., Blanco, J. & Shimmi, O. A feed-forward loop coupling extracellular BMP transport and morphogenesis in Drosophila wing. *PLoS Genet* **9**, e1003403, doi:10.1371/journal.pgen.1003403 (2013).

5 Hannezo, E. & Heisenberg, C. P. Mechanochemical Feedback Loops in Development and Disease. *Cell* **178**, 12-25, doi:10.1016/j.cell.2019.05.052 (2019).

230 6 Gilmour, D., Rembold, M. & Leptin, M. From morphogen to morphogenesis and back.
231 *Nature* **541**, 311-320, doi:10.1038/nature21348 (2017).
232 7 Ralston, A. & Blair, S. S. Long-range Dpp signaling is regulated to restrict BMP signaling
233 to a crossvein competent zone. *Dev Biol* **280**, 187-200, doi:10.1016/j.ydbio.2005.01.018
234 (2005).
235 8 Gui, J., Huang, Y. & Shimmi, O. Scribbled optimizes BMP signaling through its receptor
236 internalization to the Rab5 endosome and promote robust epithelial morphogenesis. *PLoS*
237 *Genet* (2016).
238 9 Ross, J. J. *et al.* Twisted gastrulation is a conserved extracellular BMP antagonist. *Nature*
239 **410**, 479-483, doi:10.1038/35068578 (2001).
240 10 Fristrom, D., Wilcox, M. & Fristrom, J. The distribution of PS integrins, laminin A and F-
241 actin during key stages in Drosophila wing development. *Development* **117**, 509-523 (1993).
242 11 Shimmi, O., Ralston, A., Blair, S. S. & O'Connor, M. B. The crossveinless gene encodes a
243 new member of the Twisted gastrulation family of BMP-binding proteins which, with Short
244 gastrulation, promotes BMP signaling in the crossveins of the Drosophila wing. *Dev Biol*
245 **282**, 70-83, doi:10.1016/j.ydbio.2005.02.029 (2005).
246 12 Martin, A. C. & Goldstein, B. Apical constriction: themes and variations on a cellular
247 mechanism driving morphogenesis. *Development* **141**, 1987-1998, doi:10.1242/dev.102228
248 (2014).
249 13 Daniel, E. *et al.* Coordination of Septate Junctions Assembly and Completion of Cytokinesis
250 in Proliferative Epithelial Tissues. *Curr Biol* **28**, 1380-1391 e1384,
251 doi:10.1016/j.cub.2018.03.034 (2018).
252 14 Lee, T. & Luo, L. Mosaic analysis with a repressible cell marker for studies of gene function
253 in neuronal morphogenesis. *Neuron* **22**, 451-461 (1999).

254 15 Shimada, Y., Yonemura, S., Ohkura, H., Strutt, D. & Uemura, T. Polarized transport of
255 Frizzled along the planar microtubule arrays in Drosophila wing epithelium. *Dev Cell* **10**,
256 209-222, doi:10.1016/j.devcel.2005.11.016 (2006).
257 16 Franke, J. D., Montague, R. A. & Kiehart, D. P. Nonmuscle myosin II generates forces that
258 transmit tension and drive contraction in multiple tissues during dorsal closure. *Curr Biol*
259 **15**, 2208-2221, doi:10.1016/j.cub.2005.11.064 (2005).
260 17 de Celis, J. F. Expression and function of decapentaplegic and thick veins during the
261 differentiation of the veins in the Drosophila wing. *Development* **124**, 1007-1018 (1997).
262 18 Moreno, E., Basler, K. & Morata, G. Cells compete for decapentaplegic survival factor to
263 prevent apoptosis in Drosophila wing development. *Nature* **416**, 755-759,
264 doi:10.1038/416755a (2002).
265 19 Moreno, E. & Basler, K. dMyc transforms cells into super-competitors. *Cell* **117**, 117-129,
266 doi:10.1016/s0092-8674(04)00262-4 (2004).
267 20 Adachi-Yamada, T. & O'Connor, M. B. Morphogenetic apoptosis: a mechanism for
268 correcting discontinuities in morphogen gradients. *Dev Biol* **251**, 74-90 (2002).
269 21 Affolter, M. & Basler, K. The Decapentaplegic morphogen gradient: from pattern formation
270 to growth regulation. *Nat Rev Genet* **8**, 663-674, doi:10.1038/nrg2166 (2007).
271 22 Restrepo, S., Zartman, J. J. & Basler, K. Coordination of patterning and growth by the
272 morphogen DPP. *Curr Biol* **24**, R245-255, doi:10.1016/j.cub.2014.01.055 (2014).
273 23 Bowling, S., Lawlor, K. & Rodriguez, T. A. Cell competition: the winners and losers of
274 fitness selection. *Development* **146**, doi:10.1242/dev.167486 (2019).
275 24 Gui, J. *et al.* Coupling between dynamic 3D tissue architecture and BMP morphogen
276 signaling during Drosophila wing morphogenesis. *Proc Natl Acad Sci U S A*,
277 doi:10.1073/pnas.1815427116 (2019).

278 25 Milan, M., Campuzano, S. & Garcia-Bellido, A. Cell cycling and patterned cell proliferation
279 in the Drosophila wing during metamorphosis. *Proc Natl Acad Sci U S A* **93**, 11687-11692
280 (1996).
281 26 Serpe, M. *et al.* The BMP-binding protein Crossveinless 2 is a short-range, concentration-
282 dependent, biphasic modulator of BMP signaling in Drosophila. *Dev Cell* **14**, 940-953,
283 doi:10.1016/j.devcel.2008.03.023 (2008).
284 27 Pinheiro, D. & Bellaiotache, Y. Mechanical Force-Driven Adherens Junction Remodeling
285 and Epithelial Dynamics. *Dev Cell* **47**, 391, doi:10.1016/j.devcel.2018.10.021 (2018).
286 28 Irvine, K. D. & Shraiman, B. I. Mechanical control of growth: ideas, facts and challenges.
287 *Development* **144**, 4238-4248, doi:10.1242/dev.151902 (2017).
288 29 Sivakumar, A. & Kurpios, N. A. Transcriptional regulation of cell shape during organ
289 morphogenesis. *J Cell Biol* **217**, 2987-3005, doi:10.1083/jcb.201612115 (2018).
290 30 Heer, N. C. & Martin, A. C. Tension, contraction and tissue morphogenesis. *Development*
291 **144**, 4249-4260, doi:10.1242/dev.151282 (2017).
292 31 Rauzi, M., Lenne, P. F. & Lecuit, T. Planar polarized actomyosin contractile flows control
293 epithelial junction remodelling. *Nature* **468**, 1110-1114, doi:10.1038/nature09566 (2010).
294 32 Buttitta, L. A., Katzaroff, A. J., Perez, C. L., de la Cruz, A. & Edgar, B. A. A double-
295 assurance mechanism controls cell cycle exit upon terminal differentiation in Drosophila.
296 *Dev Cell* **12**, 631-643, doi:10.1016/j.devcel.2007.02.020 (2007).
297 33 Ashburner, M., Golic, K. G. & Hawley, R. S. Drosophila: A Laboratory Handbook, Second
298 Edition (Cold Sprig Habor, NY: Cold Spring Habor Press). (2004).
299 34 Amoyel, M. & Bach, E. A. Cell competition: how to eliminate your neighbours.
300 *Development* **141**, 988-1000, doi:10.1242/dev.079129 (2014).

301

302 **Materials and methods**

303 **Fly genetics**

304 *UAS-mCD8::GFP* (#5137) and *en-Gal4* (#30564) were obtained from the Bloomington *Drosophila*
305 Stock Centre. *UAS-tkv*$^{Q253D}$ and *cv*$^{70}$ were described previously[8,11]. *Shg::GFP* was obtained from H.
306 Ohkura[15], *MyoII::RFP* from R. Le Borgne[13], *UAS-MyoII-DN* from D. Kiehart[16] and *sqh-*
307 *GAP43::mCherry* from A. Martin[31]. Flies were raised at 25°C unless otherwise stated. Populations
308 of mixed sex were used except for when using *yw*, where females were selected, and experiments
309 involving *crossveinless* where only males were used. The age of pupal wingsat dissection are given
310 at developmental timepoints equivalent to 25 $^{o}$C. Calculations for relative developmental timing at
311 18 $^{o}$C, 25 $^{o}$C and 29 $^{o}$C were based on previously published data and rounded to the nearest
312 hour[32,33]. For experiments using *en-Gal4* pupae were raised at 18°C for 22 hours after pupariation,
313 and then shifted to 29°C for either 10 (Fig. 3a, Extended Data Fig. 2a, b) or 12 (Extended Data Fig.
314 3a) hours before dissection and fixation. For clone generation larvae were raised at 25°C for 3-4
315 days AEL (or 18°C for 6-7 days AEL), before being heat shocked in a 37°C water bath for 1 hour.
316 Vials containing larvae were then placed in 18°C until at the white pre-pupal stage when they were
317 transferred to 29°C for 21 hours before dissection and fixation. For time lapse imaging pupae were
318 raised at 25°C until 17 hours after the pre-pupal stage. They were then moved to room temperature
319 for one hour during which time windows were cut into the pupal case and pupae mounted before
320 being imaged as previously described[24].

321

322 **Full genotypes**

323 Fig. 1d, 4a,: *yw*

324 Fig. 1f and Extended Data Fig. 3b: *yw; ubi-shg::GFP,* or *cv*$^{70}$*; ubi-shg::GFP*

325 Fig. 1g and Extended Data Fig. 1a: *MyoII::RFP,* or *MyoII::RFP, cv*$^{70}$

326 Fig. 2a and Suppl videos 1-3: *ubi-shg::GFP/sqh-Gap43::mCherry*

327 Fig. 3a and Extended Data Fig. 2a: *en-Gal4/UAS-mCD8::GFP; tubP-Gal80$^{ts}$,* or *en-Gal4/UAS-*
328 *MyoII-DN; tubP-Gal80$^{ts}$*

329 Fig. 3c and Extended Data Fig. 2c and d: *hs-Flp; tubP-Gal4 UAS-mCD8::GFP/UAS-MyoII-DN;*
330 *tubP-Gal80 FRT$^{82B}$ /FRT$^{82B}$*

331 Extended Data Fig. 1b: *hs-Flp/tubP-Gal80$^{ts}$, MyoII::RFP; tubP-Gal4 UAS-mCD8::GFP/UAS-*
332 *tkv$^{Q253D}$ (caTKV); tubP-Gal80 FRT$^{82B}$ /FRT$^{82B}$*

333 Extended Data Fig. 2b: *cv$^{70}$; en-Gal4/+; tubP-Gal80$^{ts}$*, or *cv$^{70}$;en-Gal4/UAS-MyoII-DN; tubP-*
334 *Gal80$^{ts}$*

335 Extended Data Fig. 3a: *en-Gal4/sqh-Gap43::mCherry; tubP-Gal80$^{ts}$*, or *en-Gal4/UAS-MyoII-DN,*
336 *sqh-Gap43::mCherry; tubP-Gal80$^{ts}$*

337

338 **Immunohistochemistry**

339 Pupae were fixed in 3.7% formaldehyde (Sigma-Aldrich) for 2 nights at 4°C before dissecting the
340 pupal wings, removing the cuticle and blocking with Normal Goat Serum (10%) overnight. Both
341 primary and secondary antibody incubations also took place overnight at 4°C. The following
342 primary antibodies were used: mouse anti-DLG1 [1:40; Developmental Studies Hybridoma Bank
343 (DSHB), University of Iowa] and rabbit anti-phospho-SMAD1/5 (1:200; Cell Signaling
344 Technologies). Secondary antibodies were anti-rabbit IgG Alexa 568 (1:200, Invitrogen), anti-
345 mouse IgG Alexa 647 (1:200; Life technologies), anti-rabbit IgG Alexa 647 (1:200; Life
346 technologies). F-actin was stained with Alexa 488 conjugated phalloidin (1:200; Life technologies).

347

348 **Imaging and Image Analysis**

349 Confocal images and time lapse imaging was conducted using a Leica SP8 STED confocal
350 microscope. Time lapse images were processed using Imaris v9.1.2 (Bitplane/Oxford Instruments)
351 and snapshots segmented by hand in Image J/Fiji. All other images processed and analysed using
352 Fiji. All images, including time lapse snap shots are maximum composites. Median filter applied to
353 all pMad images in Fiji to remove noise. The heatmap was generated using the ROI color coder
354 plugin, part of the BAR collection of ImageJ.

355 The number of pMad positive cells within the PCV field was calculated by first excluding adjacent
356 LV nuclei by marking the predicted trajectory of the LV–PCV boundary by drawing across from
357 the edge of L4 and L5 on either side of the PCV. All pMad positive nuclei (regardless of intensity
358 of stain) between these lines were then counted. Z projections of median filtered images were used
359 for quantification, using the stacks for reference.

360 The basal sizes of field cells were analysed using individual slices of stacks in Fiji. Cell outlines on
361 the basal side of cells that showed pMad staining in the nucleus were traced and measured. The
362 most basal slice where the cell outline was clear was used for each cell. Cells at the centre and
363 posterior portion of the PCV were analysed. Cells that run along the edge of the PCV field were
364 designated peripheral cells.

365 All representative images are representative of at least 3 biological replicates.

366

367 **Statistics**

368 Statistical analyses were performed using GraphPad Prism software (v.8.3.0, GraphPad). The
369 number for all quantified data is indicated in the figure legends. All *P* values were calculated using
370 a two-sided Mann-Whitney test and specified in the figure legends and in the corresponding plots.

371

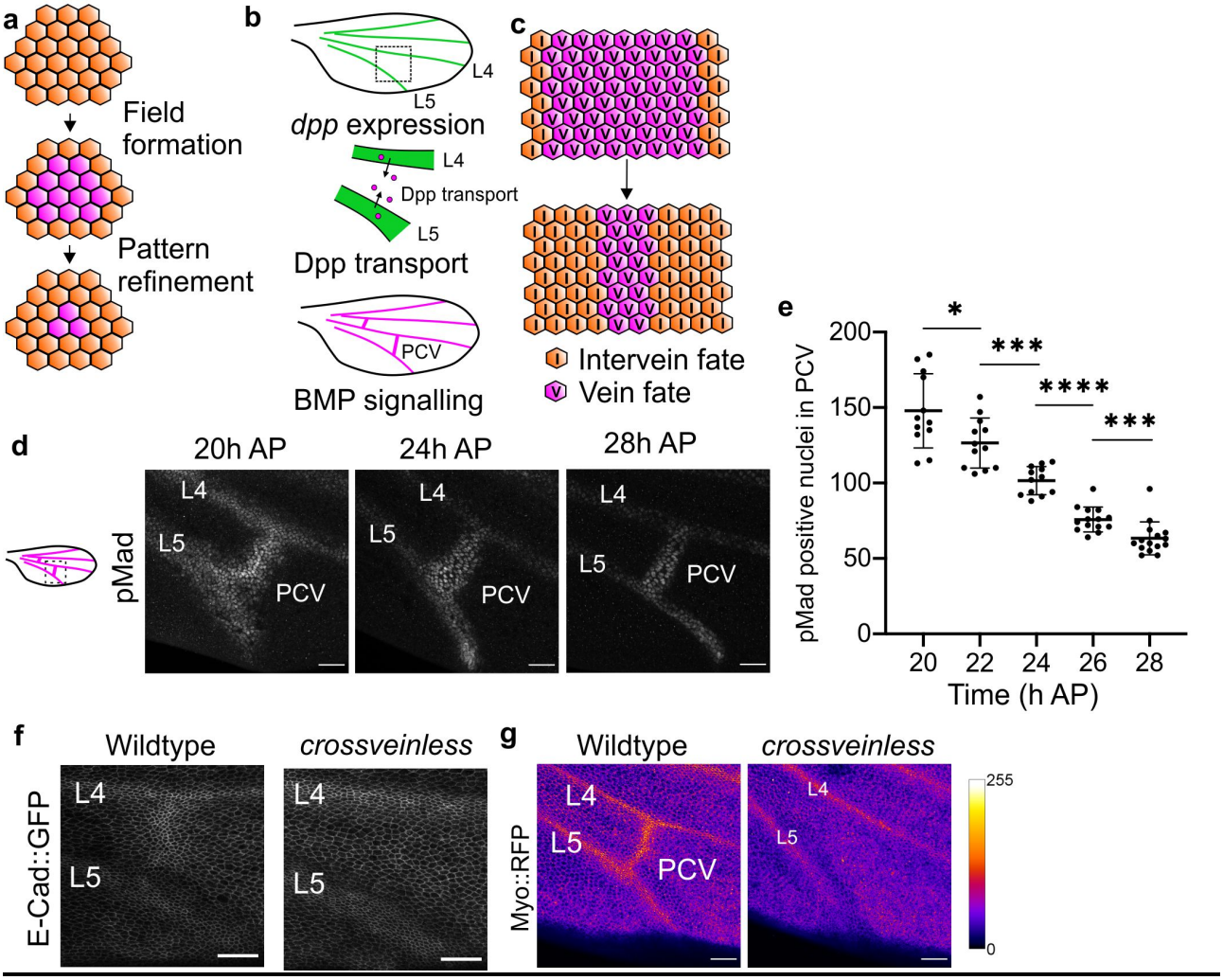


**Fig. 1: The PCV field refines during vein patterning and morphogenesis. a,** Schematic depicting the refinement of developmental patterns from an initial field to cells committing to a fate. **b,** The expression pattern and signalling pattern of the BMP ligand Dpp in the developing pupal wing. L4, L5, and PCV denote longitudinal veins 4, 5, and posterior crossvein, respectively. Top: *dpp* mRNA (green) is expressed in longitudinal veins but not in crossveins during early pupal stages. Middle: Schematic model of Dpp/BMP ligand transport from the longitudinal veins into PCV. Bottom: BMP signalling (magenta) is detected at all wing vein primordia including longitudinal veins and crossveins. **c,** Schematic depicting the refinement of the BMP signalling pattern in the PCV field. **d,** BMP signalling (shown by pMad) in the PCV field of wildtype *yw* pupal wings at 20 h, 24 h and 28 h AP. Left: Schematic of pupal wing. Approximate position of imaging is shown as a square. Median filter applied. **e,** The number of cells in which BMP

signalling is occurring during the refinement period. Sample sizes are 12 (20 h), 12 (22 h), 12 (24 h), 14 (26 h) and 15 (28 h). *$P$ = 0.0252, 22-24h: ***$P$ = 0.0005, ****$P$ < 0.0001, 26-28h: ***$P$ = 0.0002. Data are mean ± s.d. and were analysed by two-sided Mann-Whitney test. **f,** E-Cadherin::GFP in the PCV region in wildtype (left) and *crossveinless* mutant (right) pupal wings at 24 h AP. Apical cell shapes are highlighted by max composite of E-Cadherin:GFP. **g,** Heatmap of the apical intensity of MyoII::RFP in cells of the PCV region in wildtype (left) and *crossveinless* mutant (right) pupal wings at 24h AP. The distribution of MyoII is shown by max composite of apical sections. Scale bars: 25 µm for **d**, **f** and **g**.

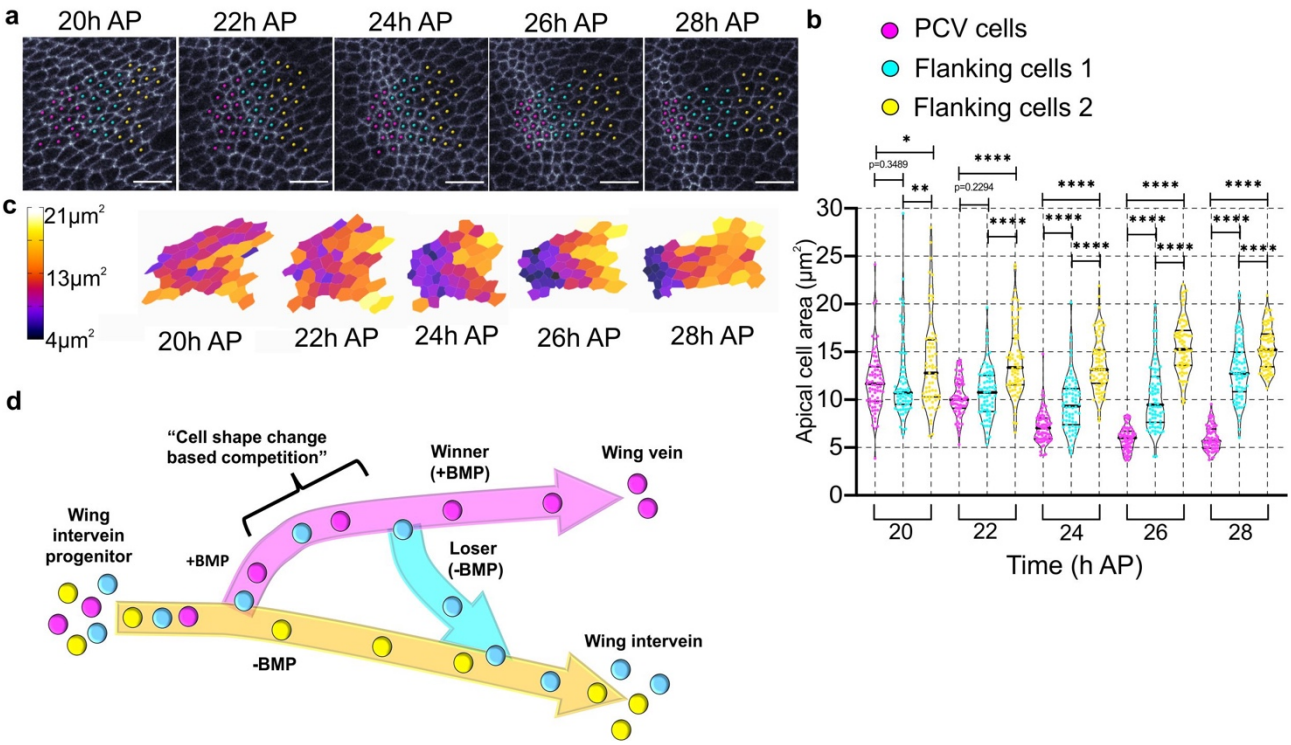


**Fig. 2: Changes in cell shape are dynamic and transient during pattern refinement. a,** Time-lapse images of E-Cadherin::GFP in the PCV region at 20 h, 22 h, 24 h, 26 h and 28 h AP. Three clusters of cells are marked. Future PCV cells (magenta) show progressive apical constriction. Cells immediately adjacent to future PCV cells (cyan) show transient apical constriction during 22 h and 26 h AP before reverting to an intervein-like structure. Cells further from future PCV cells (yellow) do not show apical constriction. PCV cells are categorised by their shape at 28 h AP and flanking categories by their relative position and shape at 28 h AP. Scale bars: 10 µm. **b,** Apical size of PCV cells and their neighbours during the refinement period. N=75 cells per category (15 cells tracked per category in each wing, for 5 wings). Violin pots show median, and 25th and 75th percentiles. Data from 5 independent time-lapse images. Each data point [PCV cells: magenta, cells adjacent to PCV (Flanking cells 1): cyan, cells further from PCV (Flanking cells 2): yellow] represents one cell. $*P = 0.0185$, $**P = 0.0071$, $****P < 0.0001$. Data were analysed by two-sided Mann-Whitney test. **c,** Heat map showing the changes in apical area of cells of the PCV field. The heatmap was produced using the ROI color coder plugin, part of the BAR collection of ImageJ. **d,** Schematic of changes in fate path during PCV patterning. Cells that are initially on a vein fate path (cyan) lose

409 competence during patterning, and move outwith the vein fate path (magenta) into the intervein fate
410 path (yellow). More details about “cell shape change based competition” are described in Fig. 3 and
411 Extended Data Fig. 4.

412

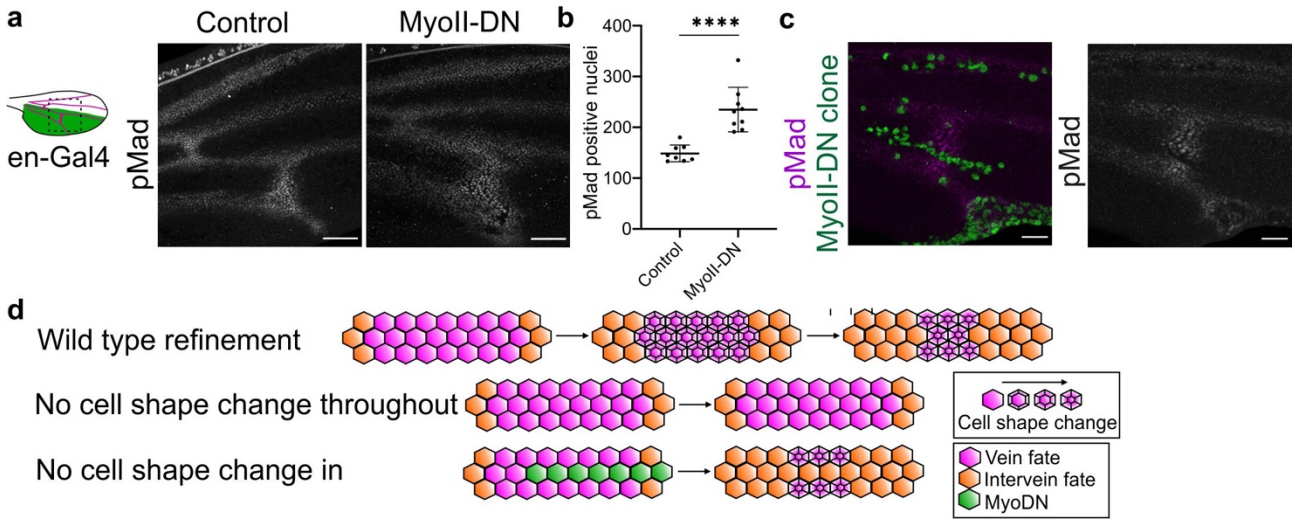


**Fig. 3: Loss of MyoII activity has context specific effects on BMP signalling pattern refinement. a,** pMad expression in the PCV region in control (middle, *en > mCD8::GFP*) and MyoII attenuated pupal wings (right, *en > MyoII-DN*) at 25 h AP. MyoII-DN was expressed throughout the posterior wing by *en-Gal4* for 10 hours prior to dissection. Approximate position of *en* expression is shown as green in schematic of pupal wing (left). Median filter applied. **b,** Number of cells in which BMP signalling is occurring (and thus are within the PCV field) in the PCV of 25h AP pupal wings. N= 8 (control) and 9 (MyoII-DN)**.** ****$P < 0.0001$. Data are mean ± s.d. and were analysed by two-sided Mann-Whitney test. **c,** Effects of clonal expression of MyoII-DN within a subset of cells of the PCV field. pMad staining (magenta) MyoII-DN expressing clones (green) at 24 h AP (left), or pMad staining alone (white, right). Median filter applied to pMad staining. Scale bars: 50 µm for **a** and 25 µm for **c**. **d,** Top: Schematic depicting model of wild type pattern refinement whereby loss of cell shape changes from cells at the edge of the PCV field results in their exclusion from the field (by loss of BMP signalling and thus cell fate). Middle: Loss of MyoII activity and cell shape change throughout the PCV blocks refinement**.** Bottom: Loss of MyoII activity in a subset of PCV cells can lead to loss of signal and fate (ectopic refinement).

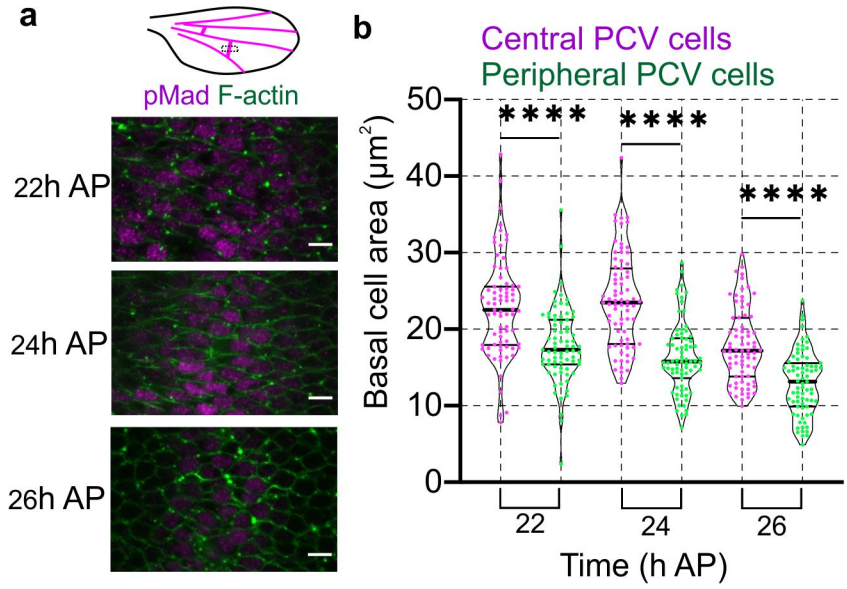


**Fig. 4: Central cells in the PCV field that retain vein fate throughout refinement are more basally expanded than their peripheral neighbours. a,** Max composites showing basal cell shape of PCV field cells during the refinement period. pMad staining (magenta) and F-actin (green) at 22h AP, 24h AP and 26h AP (left). Top: schematic of pupal wing. Approximate position of imaging is shown as a dotted line. Median filter applied to pMad staining. **b,** Basal cell areas of peripheral cells are smaller than those of central cells during refinement. N = 75 (15 cells per wing, data from 5 wings pooled). Violin pots show median, and 25th and 75th percentiles. Each data point (central PCV cells: magenta, peripheral PCV cells: green) represents one cell. ****$P < 0.0001$. Data were analysed by two-sided Mann-Whitney test.

441 **Extended Data figures**

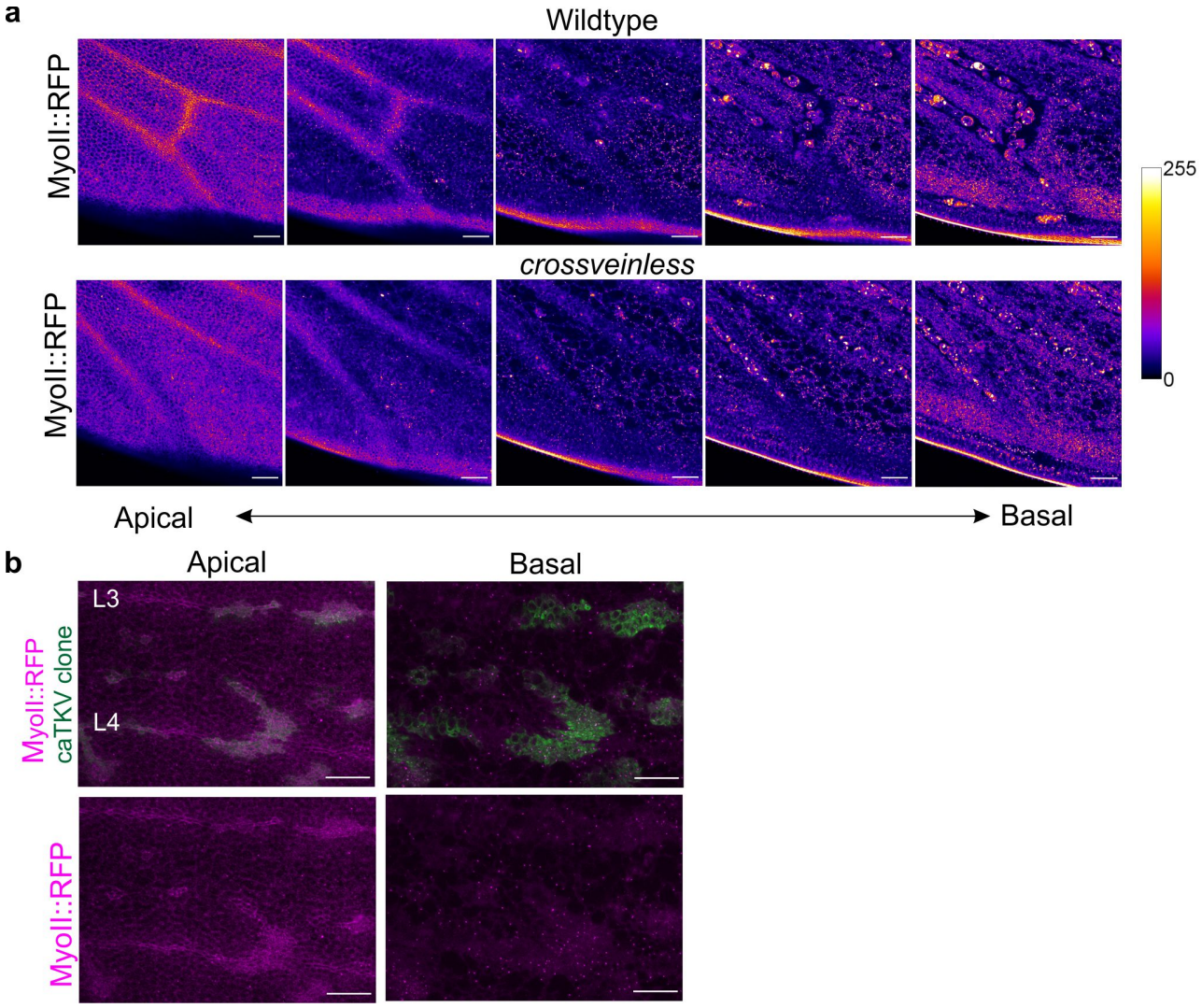


442

443 **Extended Data Fig. 1: a,** MyoII-RFP localisation throughout progressive apical to basal

444 projections of PCV field and intervein cells in wild type and *crossveinless* mutant 24 h AP pupal

445 wings. Max composites of five different sequential sections of the pupal wing along the apicobasal

446 axis. Same tissues shown as in Fig 1g. **b,** Apical and basal max composites showing MyoII-RFP

447 localisation in ectopic clones expressing constitutively active BMP receptor Tkv (25 h AP). Scale

448 bars: 25 µm for **a** and **b**.

449

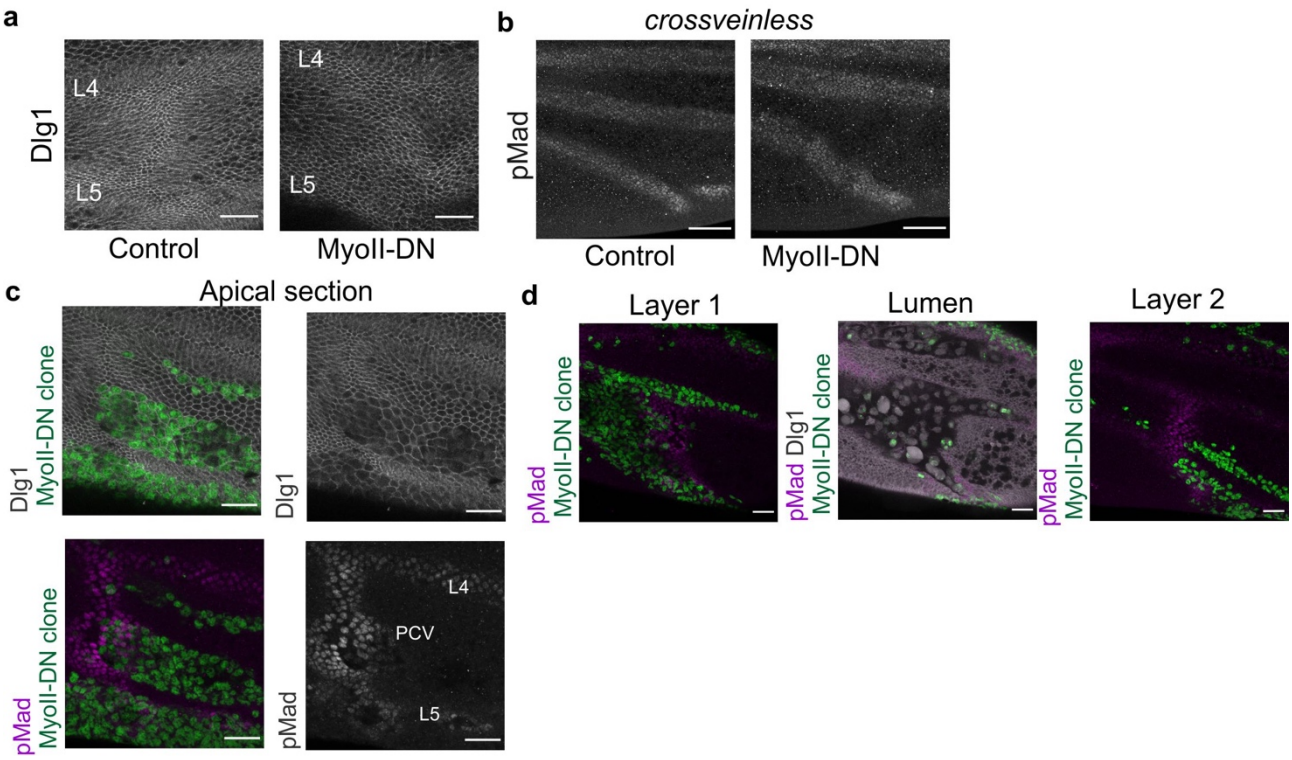


**Extended Data Fig. 2: a** Apical cell shape (Dlg1) in the PCV region in control (left, *en* > *mCD8::GFP*) and MyoII attenuated pupal wings (right, *en* > *MyoII-DN*) at 25 h AP. From the same dataset as Fig 3a. **b** pMad expression in the PCV region in control (left, *en* ) and MyoII attenuated pupal wings (right, *en* > *MyoII-DN*) at 25 h AP in a *crossveinless* background. Median filter applied. **c** Effects of clonal expression of MyoII-DN within a subset of cells of the PCV field on pMad staining (magenta - bottom) and apical cell size (Dlg1 – top) at 25 h AP. MyoII-DN expressing clones are marked by GFP (green). Note that large clones contain cells that both lose and retain the BMP signal despite attenuation of MyoII activity. Median filter applied to pMad staining. **d** Effects of large clones expressing MyoII-DN (left) that disrupt apposition of cell layers and lumen formation (middle), on the other cell layer (right). Median filter applied to pMad staining. Scale bars: 25 µm for **a**, 50 µm for **b,** and 25 µm for **c** and **d**.

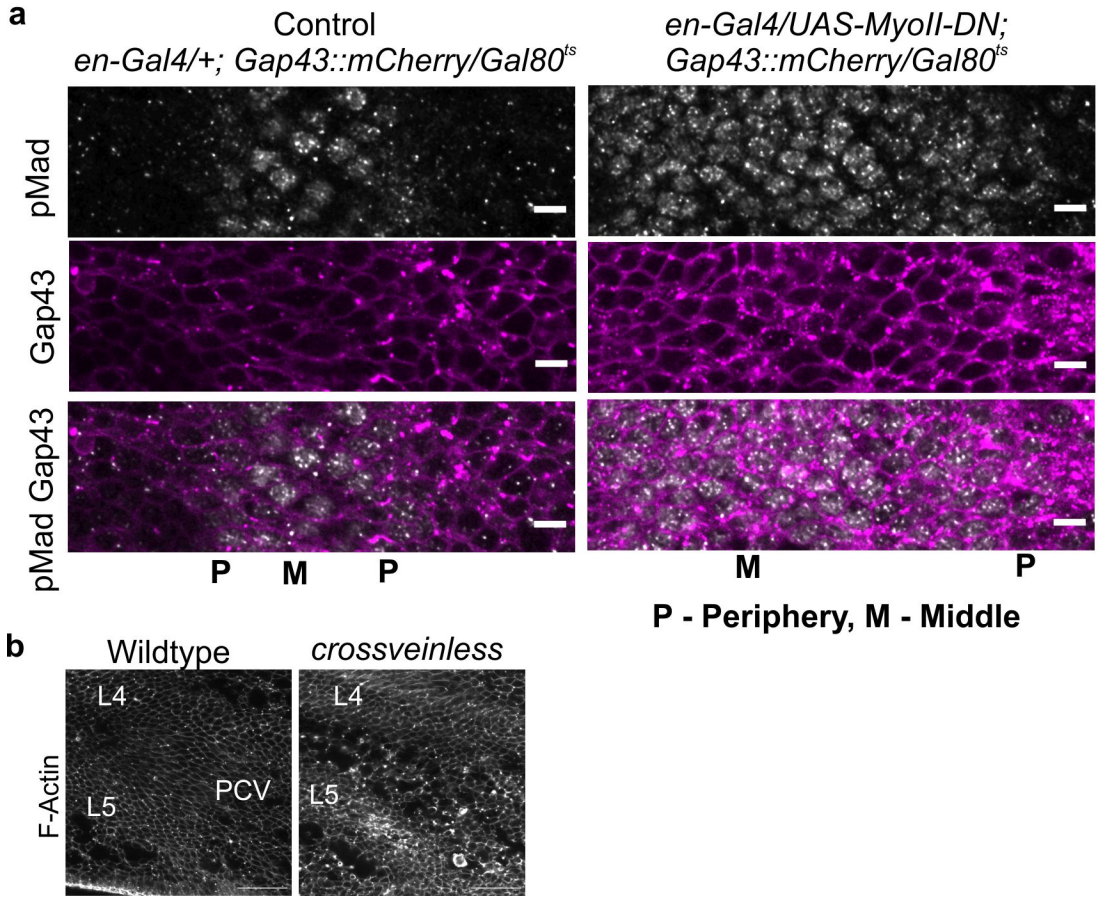


463

464 **Extended Data Fig. 3: a** Basal cell shapes (Gap43 - magenta) in the PCV field (marked by pMad –
465 white) in control (left) and MyoII attenuated pupal wings (right, *en* > *MyoII-DN*) at 26h AP. Max
466 composite of basal regions of the cells are shown. Middle and periphery of the PCV filed are
467 labelled by M and P. Median filter applied to pMad staining. **b** Basal cell size of PCV field cells in
468 wild type and *crossveinless* mutant 24 h AP wings. Wings are from the same dataset as Fig 1f.
469 Scale bars: 5 µm for **a** and 25 µm for **b**.

470

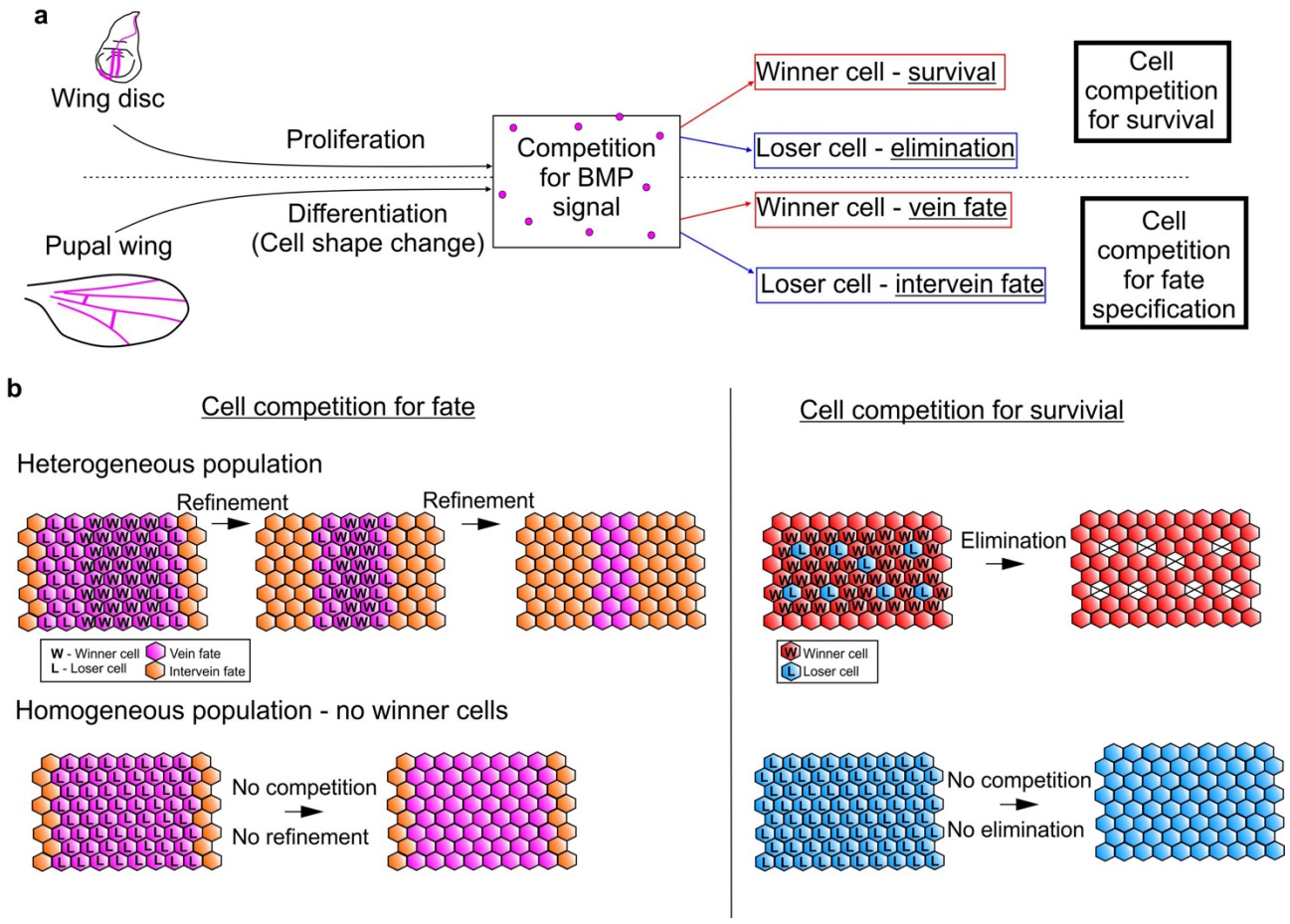


**Extended Data Fig. 4: a** Schematic showing that competition for the BMP signal in both pupal wing and wing disc can lead to cell competition. In the wing disc the outcome of competition is either elimination or survival, whereas in the pupal wing the choice is either vein or intervein fate. **b** Schematics of cell competition in homogeneous and heterogeneous populations. Top left: Schematic depicting model of wild type pattern refinement whereby loss of cell shape changes from cells at the edge of the PCV field results in their exclusion from the field (by loss of BMP signalling and thus cell fate). Bottom left: Loss of MyoII activity and cell shape change throughout the PCV blocks refinement as no competition occurs. Top right: Classical cell competition in the wing disc, where loser cells are eliminated whilst winner cells survive[23,34]. Bottom right: Loser cells can survive classical cell competition when no winner cells are present[23,34].

483 **Supplementary information**

484 **Supplementary Video 1:** Time-lapse imaging of E-Cadherin::GFP in the PCV region between 18.5
485 h and 29.5. h AP. Three clusters of cells are marked. Future PCV cells (magenta) show progressive
486 apical constriction. Cells immediately adjacent to future PCV cells (cyan) show transient apical
487 constriction during 22 h and 26 h AP and revert to intervein-like conformation. Cells distant from
488 PCV cells do not show apical constriction through the time-lapse imaging.

489

490 **Supplementary Video 2:** Time-lapse imaging of E-Cadherin::GFP in the PCV region between 24 h
491 and 28 h AP. Cells marked by magenta and cyan show apical constriction at 24h AP. In contrast,
492 cells only marked by magenta maintain apical constriction at 28h AP, suggesting that cells marked
493 by cyan fail to maintain vein-like morphogenesis.

494

495 **Supplementary Video 3:** Time-lapse imaging of E-Cadherin::GFP in the PCV region between 19h,
496 and 21 h AP prior to apical constriction of future vein cells. Please note that future PCV (magenta)
497 and intervein cells (cyan) are within the same cell lineage at the early PCV morphogenesis.